

pubs.acs.org/acscatalysis Research Article

Kinetic Evaluation of Deactivation Pathways in Methanol-to-Hydrocarbon Catalysis on HZSM-5 with Formaldehyde, Olefinic, Dieneic, and Aromatic Co-Feeds

Brandon L. Foley, Blake A. Johnson, and Aditya Bhan*



Cite This: ACS Catal. 2021, 11, 3628-3637



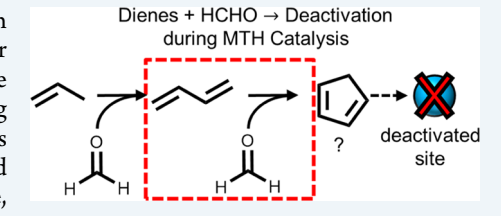
ACCESS

Metrics & More

Article Recommendations

s Supporting Information

ABSTRACT: Formaldehyde (HCHO), formed *in situ* by transfer dehydrogenation of methanol in methanol-to-hydrocarbon (MTH) conversion, reacts with other organic species including olefins, dienes, and aromatics to cause deactivation. The propensity of these formaldehyde-mediated pathways to cause deactivation during MTH catalysis is evaluated using site-loss selectivity and yield as numerical assessors of catalyst deactivation. The site-loss selectivity of HCHO with 0.2 kPa HCHO and 12 kPa CH₃OH at 673 K decreases by 80% when co-feeding 1 kPa propylene, increases by 2× when co-feeding toluene, and increases by 150× when co-feeding 1,3-



butadiene, suggesting that olefins react with HCHO in nondeactivating pathways, while aromatics and dienes react with HCHO in pathways that lead to deactivation. Further, dienes have a much higher propensity than aromatics to cause deactivation via HCHO-mediated reactions when compared on a molar basis, suggesting that dienes may be critical intermediates in HCHO-mediated deactivation pathways. This is corroborated by evidence that the site-loss selectivity of HCHO increases with increasing HCHO cofeed pressure, implying that prevalent deactivation pathways are higher order in HCHO than predominant competing nondeactivation pathways. Plausibly this occurs because HCHO reacts with itself or with a HCHO-derived species en route to deactivation, such as a diene or an aromatic, which are known products of HCHO-mediated pathways during MTH catalysis. Therefore, dienes along with HCHO should be considered as critical intermediates in fomenting deactivation in MTH catalysis and strategies to eliminate polyunsaturated species and/or intercept reaction sequences of these intermediates with HCHO will likely enhance catalyst lifetime during MTH catalysis.

KEYWORDS: chemical transients, methanol-to-hydrocarbon conversion, deactivation, formaldehyde, butadiene

1. INTRODUCTION

Formaldehyde (HCHO), formed in transfer dehydrogenation of methanol, has been implicated in shifting product selectivity toward unsaturated species, including polycyclic aromatic species that cause deactivation of zeolite/zeotype materials during methanol-to-hydrocarbon (MTH) catalysis. 1-12 The network of reaction pathways that describes HCHO-mediated deactivation is, however, not yet well understood. Polycyclic aromatics formation that results in deactivation of solid-acid zeolite/zeotype catalysts during hydrocarbon/oxygenate chemistry at MTH-relevant reaction temperatures is categorized on the basis of three general mechanisms (see Scheme 1): (i) alkylaromatic mechanism, (ii) diphenylmethane mechanism, and (iii) diene oligomerization mechanism.¹³ The precise mechanism and relative importance of each of these deactivation pathways depends on the specific chemistry and relative rates of reactions, which vary with reaction conditions and zeolite topology. $^{13-18}$ In mechanism (i), a benzenium ion undergoes alkyl-chain growth and eventual dehydrocyclization to form polycyclic aromatic species. 13 An analogous HCHOmediated alkylaromatic mechanism was proposed by Hwang and Bhan for MTH on CHA zeolite/zeotype materials as a potential HCHO-mediated deactivation pathway, where

dehydrative alkylation of aromatics with HCHO forms a benzenium ion that can undergo secondary reactions to form polycyclic aromatics species via mechanism (i) (see Scheme 2(i)). ¹² In the diphenylmethane (DPM) mechanism (mechanism (ii)), a benzyl cation undergoes electrophilic substitution with an aromatic to form DPM, which undergoes dehydrogenative coupling to form polyaromatic species. ¹³ This mechanism was proposed as a potential HCHO-mediated deactivation pathway during MTH catalysis by Martinez-Espin et al., ¹⁹ who observed methyl—DPMs during MTH catalysis with benzene co-feeds, and DPM has been demonstrated to be the highest selectivity product of HCHO condensation with benzene on HZSM-5 from 363 to 393 K. ²⁰ Martinez-Espin et al. ¹⁹ proposed that HCHO alkylation of aromatics forms an aryl alcohol that can undergo dehydrative benzylation to form

Received: December 5, 2020 Revised: February 16, 2021



ACS Catalysis pubs.acs.org/acscatalysis Research Article

Scheme 1. Polycyclic Aromatic Formation Pathways on Solid Acid Catalysts^a

$$(i) \bigcirc + \bigcirc -4H$$

$$(ii) \bigcirc + \bigcirc -4H$$

$$(iii) \bigcirc + \bigcirc -4H$$

$$(iii) \bigcirc + \bigcirc -4H$$

Scheme 2. Proposed HCHO-Mediated Deactivation Pathways during MTH Catalysis^a

^aScheme (i) is adapted with permission from ref 12. Copyright (2017 Elsevier).

DPM, which can either form poly(DPM) by homologation or undergo dehydrogenative coupling to form polycyclic aromatic species (Scheme 2(ii)). In mechanism (iii), dienes, especially cyclopentadienes, which have a propensity to form organic deposits in zeolites and other solid-acid catalysts, 13,21-24 oligomerize to form polycyclic aromatics. Polyenes have recently been identified as critical intermediates for polycyclic aromatics formation during MTH catalysis on CHA zeolite catalysts using Kerr-gate Raman spectroscopy.²⁵ Dienes, including cyclopentadienes, are observed during MTH catalysis and noncyclic dienes are products of Prinscondensation between HCHO and olefins on solid acid catalysts (Scheme 2(iiia)), 10,26-28 and we further propose that highly reactive cyclopentadiene species can be formed by dehydrative reaction of HCHO with 1,3-butadiene via a 2,4diene-1-ol intermediate (Scheme 2(iiib)). Cyclopentadienes have been shown to be active hydrocarbon pool chain carriers, ²⁹⁻³² and a recent report by Wang et al. ³³ postulates that reactions between cyclopentadienes and aromatics lead to the formation of polycyclic aromatics in HSSZ-13 based on π bond interactions observed in solid-state two-dimensional NMR spectroscopy. It has also been demonstrated previously that acid-catalyzed reactions between aromatics and dienes lead to the formation of alkenyl-aromatics and diarylalkanes, which are intermediates in mechanism (i) and (ii) in Scheme 1, respectively.^{34,35} Close proximity between cyclopentadiene and aromatics was not observed on HZSM-5 zeolite catalysts,

which Wang et al.³³ suggest may be why HZSM-5 has a lower susceptibility to form polycyclic aromatics than other MTH catalysts. Likely many different pathways simultaneously contribute to deactivation during MTH catalysis, but it is of interest to identify and understand the prominent deactivation pathways under MTH reaction conditions.^{14,36} We investigate the propensity of each deactivation pathway on HZSM-5 during MTH catalysis by measuring the site-loss yield and selectivity,³⁷ which we defined previously as model agnostic metrics of deactivation, utilizing reactant co-feeds.

The definitions for the metrics of yield, selectivity, and rate of deactivation for catalytic processes are based on treating active sites as species that are consumed stoichiometrically in deactivation reactions.³⁷ These metrics are termed the site-loss yield, selectivity, and rate defined as eqs $1-3^{37}$

site-loss yield =
$$-\frac{d\tau}{dt}$$
[=] $\frac{\text{mol sites lost}}{\text{mol reactant fed}}$ (1)

site-loss selectivity =
$$-\frac{1}{X}\frac{d\tau}{dt}$$
 [=] $\frac{\text{mol sites lost}}{\text{mol reactant consumed}}$ (2)

site-loss rate =
$$-\frac{1}{\tau} \frac{d\tau}{dt} [=] \frac{\text{mol sites lost}}{\text{s mol sites}}$$
 (3)

where X is the conversion, τ is the contact time, defined as the number of sites divided by the molar reactant flow rate, and t is time. These metrics are quantitative, do not invoke assumptions regarding linear or exponential changes in rates

^aAdapted with permission from ref 13. Copyright (2001 Elsevier).

with time or conversion, and enable the study of deactivation reactions with minimal assumptions regarding the precise deactivation and product-forming mechanisms. These metrics are assessed instantaneously, i.e., at a specified conversion or contact time, in reaction systems that exhibit nonselective deactivation, which is when conversion changes as a function of time exclusively because the contact time is decreasing with time on stream as active sites are consumed by deactivation reactions. For reaction systems that deactivate nonselectively, the conversion is written as eq 4^{37–39}

$$X = X(\tau(t)) \tag{4}$$

By taking the derivative of both sides of eq 4 and rearranging, we derive an equation for the site-loss yield (eq 5)^{37,39}

$$-\frac{\mathrm{d}\tau}{\mathrm{d}t} = -\frac{\mathrm{d}X}{\mathrm{d}t} \left(\frac{\mathrm{d}X}{\mathrm{d}\tau}\right)^{-1} \tag{5}$$

The site-loss yield, $-d\tau/dt$, cannot be directly measured but is related to two measurable quantities, the change in conversion with time on stream, dX/dt, and the change in conversion (in the absence of deactivation) with contact time, $dX/d\tau$, by eq 5.

Herein, we probe the mechanisms of deactivation by measuring the site-loss yield and selectivity while co-feeding formaldehyde, ethylene, propylene, 1,3-butadiene, and toluene under MTH reaction conditions on HZSM-5. The validity of eqs 4 and 5 and the methods for assessing deactivation during MTH catalysis on HZSM-5 are discussed in our previous work.³⁷ Using these methods, we assess the functional dependence of deactivation reaction rates on the partial pressure of HCHO with and without toluene co-feeds to elucidate MTH deactivation pathways and determine the propensity of olefins, aromatics, and dienes to participate in these HCHO-mediated deactivation pathways.

2. METHODS

2.1. Experimental Methods for Assessing Conversion Versus Contact Time and Conversion Versus Time on **Stream.** Formaldehyde trimers (1,3,5-trioxane, ≥99%, Sigma-Aldrich) were dissolved in methanol (Chromosolv, ≥99% purity, Sigma-Aldrich) and fed via a syringe pump (Cole Parmer 78-0100C) into a heated stream of helium carrier gas (≥99.997%, Matheson). Toluene (≥99.9, Sigma-Aldrich) was fed via a separate syringe pump into the same helium carrier gas stream. Ethylene (≥99.999%, Praxair), propylene (≥99.83%, Sigma-Aldrich), 1,3-butadiene (≥99%, Sigma-Aldrich), and helium flow rates were regulated by mass flow controllers (Brooks SLA5850). Reactant flow rates were adjusted to achieve desired contact times and reactant partial pressures for each experiment. The reactant stream was fed to a quartz tube reactor (0.4-1 cm i.d.) containing HZSM-5 (Zeolyst, CBV8014, 0.012 g) zeolite catalysts (powder, pressed, crushed, and sieved into 177-400 µm aggregates) diluted with quartz sand (~0.1 g, 2 M HNO₃ washed, rinsed with deionized water, heated to 1273 K in flowing air for 12 h). Physical and chemical characterization of the HZSM-5 catalyst used in this study to assess porosity, crystal structure, and acid site density can be found in prior reports. 37,40,41 The quartz tube reactors were heated to reaction temperature (673 K) by a resistively heated furnace (National Element FA120) equipped with a PID controller (Watlow 96). A K-type thermocouple (Omega) monitored the temperature at the axial center of the reactor bed on the outside of the quartz tube

reactor. Before each reaction, the catalyst was regenerated by oxidative thermal treatment in air (Matheson, Ultra Zero Certified, 1.67 cm³ s⁻¹) at 823 K for 6 h. The fractional conversion of methanol (X_{MeOH}) is defined such that methanol and dimethyl ether (DME) are both reactants and is based on the total carbon molar flow rate minus the molar flow rate of nonmethanol co-feeds (HCHO, ethylene, propylene, toluene, 1,3-butadiene), as shown in eq 6, where $n_{\text{C},i}$ and $\dot{n}_{i,\text{out}}$ ($\dot{n}_{i,\text{in}}$) are the carbon number and the molar effluent (influent) flow rates of species i, respectively.

$$X_{\text{MeOH}} = \frac{\sum_{i} n_{\text{C},i} \dot{n}_{i,\text{out}} - \left(2 \dot{n}_{\text{DME,out}} + \dot{n}_{\text{CH}_3\text{OH,out}} + \sum_{i=\text{co-feeds}} n_{\text{C},i} \dot{n}_{i,\text{in}}\right)}{\sum_{i} n_{\text{C},i} \dot{n}_{i,\text{out}} - \sum_{i=\text{co-feeds}} n_{\text{C},i} \dot{n}_{i,\text{in}}}$$
(6

Conversion versus contact time $(dX/d\tau)$ data were obtained by measuring the conversion at 180 s time on stream for each reactant composition at two or three different initial contact times that spanned methanol conversions ranging from ~20 to ~80%. The 180 s time on stream was chosen because it was after the initiation of the hydrocarbon pool but before substantial deactivation reduced the number of active sites in the reactor bed. In each of these experiments, the conversion was also monitored with time on stream to obtain dX/dt for each reaction condition. The reactor effluent composition was determined by a gas chromatograph (Agilent 7890) equipped with an HP-Plot/Q column (30 m \times 0.530 mm \times 40 μ m) in series with a CP-Molsieve 5 Å column (25 m \times 0.530 mm \times 40 μ m). The column outlets were connected to a thermal conductivity detector (TCD) preceding an oxidationmethanation reactor (Polyarc, Activated Research Company) in series with a flame ionization detector (FID). The reactor effluent streams were stored in 250 µL heated (373 K) stainless steel sample loops using a multiposition valve and analyzed shortly after the reaction or injected directly into the GC. The site-loss yield of methanol was calculated using eq 5. The site-loss selectivity of HCHO was calculated from the siteloss yield of methanol as shown in eq 7

site-loss selectivity of HCHO =
$$-\frac{1}{X_{\text{HCHO}}} \frac{d\tau_{\text{HCHO}}}{dt}$$

$$= \frac{\dot{n}_{\text{MeOH}}}{X_{\text{HCHO}} \dot{n}_{\text{HCHO}}} \left(-\frac{1}{\dot{n}_{\text{MeOH}}} \frac{dn_*}{dt} \right)$$

$$= \frac{\dot{n}_{\text{MeOH}}}{X_{\text{HCHO}} \dot{n}_{\text{HCHO}}} \left(-\frac{d\tau_{\text{MeOH}}}{dt} \right)$$
(7)

where $-\mathrm{d}\tau_{\mathrm{MeOH}}/\mathrm{d}t$ is the site-loss yield of methanol. The molar flow rates of methanol and formaldehyde $(\dot{n}_{\mathrm{MeOH}}, \dot{n}_{\mathrm{HCHO}})$ are known and the formaldehyde conversion (X_{HCHO}) was 100% at all conditions of interest in this study.

3. RESULTS AND DISCUSSION

Under typical MTH conditions, HCHO is formed *in situ* and reacts with other organic species formed during MTH catalysis to form polycyclic aromatic species. We probe HCHO-mediated deactivation mechanisms during MTH catalysis on HZSM-5 by co-feeding species that are representative of the MTH hydrocarbon pool: ethylene and propylene for olefins, toluene for aromatics, and 1,3-butadiene for polyunsaturated nonaromatic species. Toluene was chosen to represent aromatics because it has been demonstrated previously that co-feeding toluene during MTH catalysis on HZSM-5 alters

Table 1. Slope of Conversion Versus Contact Time, Conversion Versus Time Curves, and Site-Loss Yield with Various Co-Feeds with 12 kPa Methanol at 673 K and ~50% Conversion in Methanol

	$\mathrm{d}X/\mathrm{d} au$	$-\mathrm{d}X/\mathrm{d}t$	site-loss yield $(-d\tau/dt)$
co-feeds ^a	$mol\ MeOH\ (mol\ H^+)^{-1}\ s^{-1}$	10^{-6} s^{-1}	μ mol $\mathrm{H_{lost}^{+}}$ mol $\mathrm{MeOH^{-1}}$
no co-feed	1.16	1.0	0.9
propylene	1.25	5.7	4.6
toluene	1.19	15	12
НСНО	1.31	51	39
1,3-butadiene	1.23 ^b	770	630
propylene + HCHO	1.67	8.8	5.3
propylene + toluene	1.15	12	10
ethylene + HCHO	1.28	36	29
toluene + HCHO	1.27	100	81
1,3-butadiene + HCHO	1.23 ^b	7200	5900
propylene + toluene + HCHO	1.12	53	47

[&]quot;Propylene, toluene, ethylene, and butadiene co-feeds are 1 kPa, and HCHO co-feed is 0.2 kPa. "Not measured. Taken as the average of all other $dX/d\tau$ values.

the product selectivity, demonstrating that it is not unduly diffusion limited under MTH conditions. ⁴⁰ By co-feeding hydrocarbon pool species with HCHO during MTH catalysis, we enhance the relative consumption of HCHO via that pathway. The comparison of site-loss yields with varying cofeeds enables us to quantitatively determine the propensity of various HCHO-mediated pathways to cause deactivation. A more detailed mathematical description of the implication of changes in site-loss yields and selectivities with varying cofeeds in integral (nondifferential) packed-bed reactors is presented in Section S1 of the Supporting Information.

The site-loss yields for each reaction condition were assessed by measuring independently the slopes of the deactivation-free conversion versus contact time curves $(dX/d\tau)$ and the conversion versus time curves (dX/dt) during MTH catalysis with formaldehyde, olefinic, dienic, and aromatic co-feeds as reported in Table 1 (see Section S2 of the Supporting Information for conversion versus contact time and conversion versus time on stream data). The slopes for conversion versus contact time data with 1,3-butadiene co-feeds were not measured because deactivation was too rapid to identify a deactivation-free conversion for each reaction condition. Instead, $dX/d\tau$ during MTH with 1,3-butadiene co-feeds are taken as the average of the $dX/d\tau$ for all other co-feed conditions shown in Table 1 (no co-feed, propylene, ethylene, toluene, HCHO, and combinations thereof), which are relatively invariant with co-feed.

By comparison of the site-loss yields with and without HCHO co-feeds from the data reported in Table 1, we observe that co-feeding 0.2 kPa HCHO increases the site-loss yield by 38 μ mol H $_{lost}^{+}$ mol MeOH $_{fed}^{-1}$ relative to no co-feed, suggesting that HCHO induces deactivation during MTH catalysis, as is expected because HCHO has been implicated as a key chemical intermediate for causing deactivation during MTH catalysis. 5-12 However, this does not provide information on which HCHO-mediated deactivation pathways are prominent during MTH catalysis. Pre-treating the catalyst in 0.2 kPa HCHO prior to MTH reaction with no co-feed did not alter the initial conversion, conversion versus time, or product selectivity, suggesting that HCHO does not deactivate the catalyst by itself, but instead must react with methanol-derived hydrocarbons to cause deactivation (see Section S3 of the Supporting Information for conversion and selectivity data). Once formed, formaldehyde can react with any species

produced during MTH catalysis, including olefins, aromatics, and dienes, and which species HCHO reacts with significantly impacts whether HCHO renders sites inactive.

The alkylaromatic and diphenylmethane deactivation mechanisms for MTH catalysis (Scheme 2(i,ii)) both require the alkylation of aromatics by formaldehyde in formaldehydeconsuming steps. To investigate the propensity of these pathways to cause deactivation during MTH catalysis, we measure the site-loss yield with both 0.2 kPa HCHO and 1.0 kPa toluene (C₇H₈) co-feeds and compare the site-loss yield at this reaction condition to the site-loss yields when co-feeding only 0.2 kPa HCHO or only 1.0 kPa C7H8 during MTH catalysis. If reaction between HCHO and aromatics is a selectivity-determining step that determines whether co-fed formaldehyde leads to the loss of active sites during MTH catalysis, then the total site-loss yield when co-feeding HCHO and C₇H₈ simultaneously will be greater than the sum of the site-loss yields when co-feeding only HCHO or only C7H8. Comparing site-loss yields of methanol with multiple co-feeds to the sum of the site-loss yields with one co-feed is necessary because HCHO and C7H8 may each lead to deactivation through independent pathways. Thus, if there are no reactions between these two species, then the site-loss yield when cofeeding these species together should equal to the sum of the site-loss yields when co-feeding them separately. However, if there are additional reactions between HCHO and C7H8 that lead to the loss of active sites, then the site-loss yield when cofeeding these species together will be greater than the sum of the site-loss yields when these species are co-fed with methanol independently in separate experiments. From Table 1, the siteloss yield for MTH catalysis with 0.2 kPa HCHO and 1.0 kPa toluene co-feeds (81 μ mol H $_{lost}^+$ mol MeOH $^{-1}$) is 30 μ mol H $_{lost}^+$ mol MeOH⁻¹ larger than the sum of the independent site-loss yields for 0.2 kPa HCHO (39 μ mol H_{lost} mol MeOH⁻¹) and 1.0 kPa toluene (12 μ mol H $_{lost}^+$ mol MeOH $^{-1}$) co-feeds. This suggests that reactions between HCHO and C7H8 are consequent in deactivation during MTH catalysis, potentially via reactions similar to those in the alkylaromatic and diphenylmethane deactivation pathways (Scheme 2(i,ii)).

In the diene-based deactivation pathway during MTH catalysis, HCHO-derived aliphatic- and cyclodienes undergo further reactions to cause deactivation (Scheme 2(iii,iv)). To investigate the propensity of dienes to cause deactivation during MTH catalysis, we co-fed 1.0 kPa 1,3-butadiene with 12

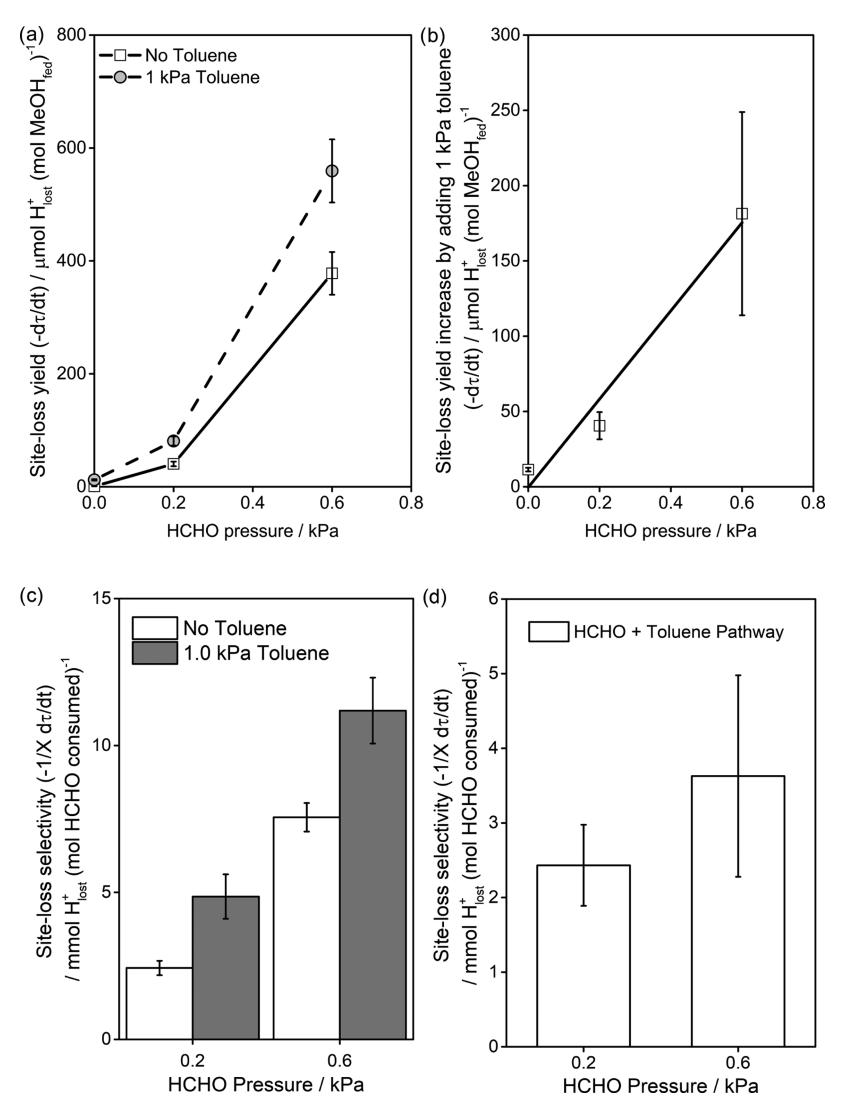


Figure 1. (a) Site-loss yield of methanol as a function of HCHO co-feed pressure with and without a 1 kPa C_7H_8 co-feed, (b) increase in the site-loss yield when adding 1 kPa C_7H_8 as a function of HCHO co-feed pressure, (c) site-loss selectivity of HCHO as a function of HCHO co-feed pressure with and without 1 kPa C_7H_8 co-feed, and (d) site-loss selectivity of the HCHO + toluene pathway if it is merely additive to the HCHO deactivation pathway, at 673 K with 12 kPa C_7H_8 co-feed, and 50% conversion of C_7H_8 conversion of HCHO.

kPa CH₃OH during MTH catalysis and measured the resulting site-loss yield. We observed that the site-loss yield increased by \sim 630 μ mol H $_{lost}^+$ mol MeOH $^{-1}$ relative to the experiment in which only CH₃OH was fed, as shown in Table 1. Further, we found that co-feeding 0.2 kPa HCHO and 1.0 kPa 1,3butadiene simultaneously resulted in a site-loss yield of 5900 μ mol H_{lost} mol MeOH⁻¹, an increase of 5200 μ mol H_{lost} mol MeOH⁻¹ relative to independent experiments in which only 0.2 kPa HCHO (39 μ mol H $_{lost}^+$ mol MeOH $^{-1}$) or 1.0 kPa 1,3butadiene (630 μ mol H_{lost} mol MeOH⁻¹) was co-fed, suggesting that reactions between HCHO and 1,3-butadiene contribute significantly to deactivation (see Table 1). The increase observed when co-feeding HCHO with 1,3-butadiene is much larger than the increase observed when co-feeding HCHO with toluene, suggesting that pathways involving dienes may contribute more significantly to deactivation during MTH catalysis than pathways involving aromatic species.

Finally, we consider the deactivation pathways between HCHO and olefins by co-reacting HCHO and propylene with methanol. We find that the total site-loss yield for HCHO and propylene simultaneously is lower than the total site-loss yield

with HCHO co-feed, suggesting that propylene decreases the propensity of HCHO to cause deactivation. This is in agreement with previous results that demonstrate that co-feeding olefins during MTH catalysis mitigates deactivation. This observation suggests that there are competing pathways for HCHO consumption: reactions between HCHO with aromatics or dienes to deactivate sites and reactions between HCHO and olefins to form nondeactivation products.

This analysis delineates the competing pathways that determine the fate of HCHO to either consume active sites and cause deactivation or be incorporated into nondeactivation products but does not shed light on the relative importance of each pathway during MTH catalysis in the absence of any cofeeds. Because formaldehyde is strongly implicated in causing deactivation during MTH catalysis, we surmise that deactivation during MTH catalysis with no co-feeds occurs via a similar mechanism to deactivation during MTH catalysis with HCHO co-feed. To elucidate the importance of the aromatics-based and diene-based deactivation pathways during MTH catalysis with HCHO co-feeds, we measure the functional dependence of the site-loss yield and selectivity on

the HCHO co-feed partial pressure. Through these measurements, we demonstrate that the reaction between HCHO and aromatics is unlikely to be the prevailing HCHO-mediated deactivation pathway during MTH catalysis with HCHO cofeeds, and we propose instead that diene-based deactivation pathways predominate.

The site-loss yield as a function of HCHO co-feed pressure with and without a 1 kPa C₇H₈ co-feed is shown in Figure 1a, and the difference between these two curves is shown in Figure 1b. The trend in Figure 1a suggests that the total site-loss yields when co-feeding HCHO or HCHO + C₇H₈ are proportional to formaldehyde concentrations to powers greater than one. The trend in Figure 1b shows that the difference between the total site-loss yield with HCHO + C₇H₈ and the total site-loss yield with just HCHO co-feed is approximately proportional to the co-feed pressure of HCHO. The cause of these trends in site-loss yields becomes clear when we consider the site-loss selectivity of HCHO, which is a measure of total moles sites lost per mole HCHO consumed during reaction, as defined in eq 2. The site-loss selectivity of HCHO increases with increasing HCHO co-feed pressure with and without a toluene co-feed, as shown in Figure 1c.

In all experiments with HCHO + C_7H_8 co-feeds, assuming a stoichiometry of 1 HCHO:1 site-loss, the site-loss selectivity of HCHO is \lesssim 1%, suggesting that most of the HCHO consumed does not lead to deactivation. The site-loss selectivity increases with increasing HCHO pressure (Figure 1c), such that (eq 8)

$$-\frac{1}{X_{\rm HCHO}}\frac{\mathrm{d}\tau_{\rm HCHO}}{\mathrm{d}t} = \frac{\nu_* r_*}{\nu_{\rm HCHO,*} r_* + \nu_{\rm HCHO,P} r_{\rm P}} \approx P_{\rm HCHO}$$
(8)

where ν_* is the number of sites lost in deactivation reactions, $\nu_{\text{HCHO},*}$ is the number of HCHO molecules consumed in deactivation reactions, $\nu_{\text{HCHO},P}$ is the number of HCHO molecules consumed in product-forming (or nondeactivation) reactions, r_* is the rate of deactivation reactions, and r_{P} is the rate of product-forming reactions. From eq 8, because the site-loss selectivity increases with increasing HCHO pressure, we conclude that (i) $\nu_{\text{HCHO},*}r_* \ll \nu_{\text{HCHO},P}r_{\text{P}}$ such that most of the HCHO is consumed in nondeactivating reactions, because if $\nu_{\text{HCHO},*}r_* \gg \nu_{\text{HCHO},*}r_{\text{P}}$, then the left-hand side of eq 8 would simplify to $\nu_*/\nu_{\text{HCHO},*}$ which is not a function of HCHO pressure, and (ii) the ratio of the rate of deactivation reactions divided by the rate of HCHO-consuming product formation reactions is approximately proportional to HCHO pressure (eq 9)

$$\frac{r_*}{r_{\rm P}} \stackrel{\propto}{\sim} P_{\rm HCHO} \tag{9}$$

Conclusion (i) further supports the hypothesis that most of the HCHO co-fed in these experiments does not lead to deactivation, as evidenced by a site-loss selectivity of HCHO of <1% when co-feeding only HCHO. Thus far, we have investigated quantitatively the impact of varying the co-feed identities on the site-loss yield (Table 1) and how the site-loss yield and selectivities change as functions of HCHO co-feed pressure (Figure 1 and eq 9). Next, we rationalize these data with potential deactivation mechanisms.

With only HCHO co-feeds, the site-loss selectivity of HCHO increases with increasing HCHO co-feed pressure (Figure 1c), from which we deduce that the site-loss rate, r_* , is higher order in HCHO pressure than the rate of the competing

nondeactivating reaction pathways, r_p (eq 9). A plausible explanation for this observation is that the rate of the deactivation pathway is order $\alpha > 1$ in HCHO, while the rate of HCHO consumption in nondeactivation pathways is order ~1 in HCHO. This implies that HCHO either reacts with itself to cause deactivation or reacts with a species whose concentration increases with increasing HCHO partial pressure, and that this reaction is in competition with a nondeactivating pathway where HCHO reacts with a species of the hydrocarbon pool whose concentration is not dependent on the HCHO co-feed partial pressure. Thus far, from the measurements of site-loss yield as a function of co-feed composition, we have identified one type of species that HCHO reacts with that does not lead to deactivation, which is the reaction between HCHO and olefins. The rate of this reaction can be described by a Langmuir-Hinshelwood-type rate function as eq 10

$$r_{\rm p} = \frac{k_{\rm p} P_{\rm HCHO} P_{\rm olefin}}{D} \tag{10}$$

where $k_{\rm P}$ is the apparent rate constant for the catalyzed reaction between HCHO and olefins on an empty catalyst surface ($\theta_* = 1$), and the denominator, D, is the typical term that arises from site-balances in Langmuir—Hinshelwood-type rate functions, which are shared by all rate functions catalyzed by the same types of active sites. Since D is the same for all reactions, we are only interested in the reaction orders with respect to each other. Thus for convenience, all reaction orders are in reference to a clean surface, where D = 1. The rate of the nondeactivating reaction between HCHO and olefins is thus first order in HCHO and first order in olefins, which during MTH catalysis are derived from methanol in the hydrocarbon pool mechanism. In contrast, by measurement of site-loss yields, we have identified two species that can react detrimentally with HCHO to cause deactivation during MTH catalysis—aromatics and dienes. Both aromatics and dienes are polyunsaturated species whose partial pressures in MTH catalysis can be enhanced by co-feeding HCHO via dehydrative Prins-condensation of HCHO with olefins to form dienes followed by subsequent chain growth and dehydrocyclization of dienes to form aromatics. 10 Thus, for these pathways, the rate of these deactivation reactions is described by eq 11

$$r_* = \frac{k_{*,\text{aromatic}} P_{\text{HCHO}} P_{\text{aromatic}} + k_{*,\text{diene}} P_{\text{HCHO}} P_{\text{diene}}}{D} \tag{11}$$

where $k_{*,\mathrm{aromatic}}$ is the apparent rate constant for the reaction between HCHO and an aromatic to cause deactivation on an empty catalyst surface, $k_{*,diene}$ is the apparent rate constant for the reaction between HCHO and a diene to cause deactivation, and the denominator, D, is the same term that arose in eq 10. Equation 11 treats the reactions of HCHO with aromatics or dienes as the selectivity-determining steps that govern whether HCHO consumes an active site. Aromatics and dienes are both products of HCHO, and thus the partial pressures of these species will correlate positively with the HCHO co-feed inlet partial pressure, and may be as much as proportional to HCHO co-feed partial pressure (i.e., $P_{\text{aromatic}} \propto$ $P_{\rm HCHO}$ and $P_{\rm diene} \propto P_{\rm HCHO}$). Because HCHO increases the partial pressures of polyunsaturated species such as aromatics and dienes, r_* is greater than first order in HCHO. Thus, when co-feeding only HCHO, the site-loss selectivity of HCHO

ACS Catalysis pubs.acs.org/acscatalysis Research Article

should increase with increasing HCHO co-feed pressure, since r_* is greater than first order in HCHO and $r_{\rm P}$ is first order in HCHO, such that their ratio $r_*/r_{\rm P}$ increases with increasing HCHO co-feed partial pressure, as is observed experimentally (Figure 1c).

Equation 11 sums the rates of two potential HCHOconsuming reaction pathways that lead to catalyst deactivation during MTH catalysis—reaction of HCHO with aromatics and reaction of HCHO with dienes. We conjecture that the siteloss selectivity of HCHO increases with increasing HCHO cofeed partial pressure because the partial pressures of aromatics and dienes both trend positively with HCHO co-feed partial pressure, such that $r_* \propto (P_{\text{HCHO}})^{\alpha}$ with $\alpha > 1$. If the aromaticbased deactivation pathway predominates in eq 11, then we can reduce the HCHO-order to unity by co-feeding aromatics with HCHO. When co-feeding aromatics, the partial pressure of aromatics along the bed will be the sum of aromatics co-fed plus the aromatics generated by reaction, such that $P_{\text{aromatics}} \approx$ $P_{\text{aromatics,in}}$, as discussed above. Thus, this eliminates the dependence of P_{aromatics} on the co-feed partial pressure of HCHO. If the aromatics-based deactivation rate predominates in eq 11, then when co-feeding aromatics, we should observe that r_* is first order in HCHO, such that r_*/r_p (or the site-loss selectivity of HCHO) is no longer a function of the HCHO co-feed pressure. However, in Figure 1c, this is not what is observed. When co-feeding 1.0 kPa toluene, the site-loss selectivity still increases with increasing HCHO co-feed pressure, suggesting that aromatics-based deactivation pathways do not predominate during MTH catalysis when cofeeding HCHO. In addition, co-feeding 0.2 kPa HCHO with 1.0 kPa C₇H₈ increases the aromatics pressure by orders of magnitude relative to co-feeding only 0.2 kPa HCHO (<0.1 kPa aromatics at <20% CH₃OH conversion, where deactivation occurs), but the site-loss selectivity only increases by a factor of ~ 2 . This suggests that the ratio r_*/r_p is nearly invariant with aromatics pressure, which is inconsistent with HCHO alkylation of aromatics being the predominant reaction that determines whether HCHO causes deactivation. Thus, we surmise that an alternative pathway, such as a diene-based deactivation pathway, is more likely to be the prevailing deactivation pathway during MTH catalysis.

Dienes are precursors to species that undergo dehydrocyclization to form aromatics and are formed as products of HCHO-olefin reactions (as illustrated in mechanism (iiia) in Scheme 2), such that diene partial pressure may be a positive order function of HCHO concentration. 5,10,12,44 If the rate r_* is predominantly the rate of site-loss via diene-based deactivation pathways, and $P_{\text{diene}} \propto (P_{\text{HCHO}})^{\alpha}$ where $\alpha > 0$ as a result of dienes being Prins-condensation products of HCHO, then the rate r* will be greater than first order in the HCHO co-feed pressure with or without a 1.0 kPa toluene co-feed, consistent with the experiment results reported in Figure 1a. Co-feeding 1.0 kPa 1,3-butadiene with 0.2 kPa HCHO results in an increase in the site-loss yield of 5200 μ mol H $_{lost}^+$ mol MeOH $_{fed}^{-1}$ compared to the 40 μ mol H_{lost}^+ mol $MeOH_{fed}^{-1}$ increase when co-feeding 1.0 kPa toluene with 0.2 kPa HCHO. This suggests that on a molar basis, dienes are much more pernicious than aromatics in transforming HCHO to deactivation products to induce site-loss. In Figure 2, we compare the site-loss selectivity of 0.2 kPa HCHO with no additional co-feed or with 1.0 kPa of toluene, propylene, or 1,3-butadiene, and note that the site-loss selectivity is less than 0.01 mol H⁺ mol HCHO⁻¹ in all cases except when co-feeding 1,3-butadiene,

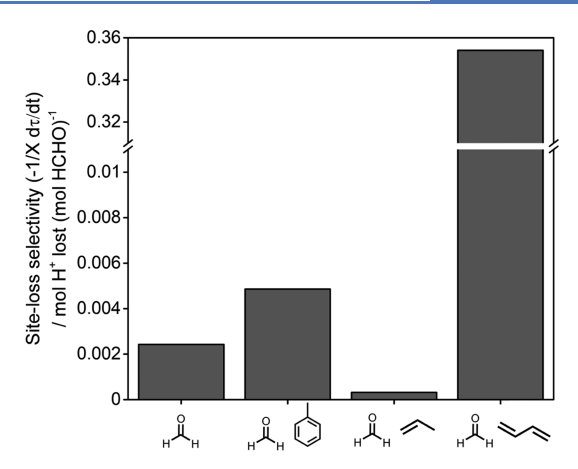


Figure 2. Site-loss selectivity of HCHO with varying co-feed combinations during methanol-to-hydrocarbon conversion on HZSM-5 at 673 K with 12 kPa CH₃OH, 50% conversion of CH₃OH, and 100% conversion of HCHO.

where the site-loss selectivity is nearly 0.4 mol H_{lost}^+ mol HCHO⁻¹. We postulate above that aromatic or diene formation may be limiting the selectivity of HCHO to siteloss as an explanation for why site-loss selectivity increases with increasing HCHO co-feed pressure. If this is the case, we expect that co-feeding the limiting species will then significantly enhance the site-loss selectivity of HCHO, which is observed when co-feeding 1,3-butadiene but not when co-feeding toluene. This result combined with the trend in site-loss selectivity with HCHO pressure when co-feeding toluene (Figure 1c and eq 9) suggests that the reactions of HCHO with aromatics are not likely the predominant deactivation pathway when co-feeding HCHO during MTH catalysis (mechanisms (i) and (ii) in Scheme 2). We instead propose that diene-mediated pathways, such as mechanisms (iiia) and (iiib) in Scheme 2, are the primary deactivation pathways at these reaction conditions.

It has been shown that high-pressure H₂ co-feeds during MTH catalysis increase catalyst lifetime on MFI, CHA, AEI, FER, and BEA zeolite/zeotype frameworks and it has been proposed that the mechanistic basis for this increased lifetime lies in the propensity of H₂ to hydrogenate dienes over olefins, evidenced by second-order rate constants that are 1–2 orders of magnitude higher for 1,3-butadiene hydrogenation compared to propylene hydrogenation. Hydrogenation of dienes may mitigate deactivation by preventing dienes from forming aromatics, or, as our data suggest, dienes are involved in critical elementary steps that cause deactivation instead of forming monocyclic aromatic intermediates. This suggests that HCHO and 1,3-butadiene react via an overall reaction to cause deactivation, possibly directly to form cyclopentadiene, which may oligomerize or react with aromatics to form polycyclic aromatic species (Scheme 1).

At the front of the reactor bed where deactivation occurs during MTH catalysis on HZSM-5, HCHO is a primary product of methanol disproportionation and transfer dehydrogenation and, at 748 K on HZSM-5, is one of the first products observed followed by light olefins that undergo subsequent reaction to form aromatics, likely through diene and cyclodiene intermediates. The observed large increase in siteloss selectivity of HCHO when co-feeding 1,3-butadiene, and the relationship between site-loss selectivity of HCHO and HCHO co-feed pressure when co-feeding 1.0 kPa toluene,

Scheme 3. Potential Deaction Pathways that Qualitatively Agree with Observed Trend in Site-Loss Yield and Site-Loss Selectivities during Methanol-to-Hydrocarbon Conversion with Co-Feeds

leads us to conclude that dienes play a critical role in deactivation during MTH catalysis. We propose that reactions between 1,3-butadiene and HCHO lead to key coke precursors by, for example, dehydrative condensation to form cyclopentadienes that either oligomerize via known acid-catalyzed coke-forming reactions¹³ or react with aromatics as proposed by Wang et al.³³ to form polycyclic species. Diels—Alder-like reactions between HCHO and dienes could also lead to the formation of oxygen-containing six-membered cyclic species⁵⁰ that can react further to form polycyclic aromatic species and may be the source of oxygen-containing coke species that are observed in HZSM-5.^{6,51}

We propose a plausible deactivation mechanism in Scheme 3 to rationalize experimental measurements of site-loss yields and selectivities. Formaldehyde is consumed in reactions with aromatics, olefins, or dienes. The dienic species can either react with HCHO to cause deactivation or with methanol and olefins to undergo further chain-growth and hydrogen-transfer reactions to form aromatics. When only HCHO is co-fed with CH₃OH, nondeactivating consumption of HCHO by reaction with olefins predominates, and a small amount of HCHO is consumed via reaction with dienic species to consume active sites, as evidenced by site-loss selectivities of less than 0.01 mol H_{lost} mol HCHO. Dienic species are formed from HCHO, and thus the selectivity of this pathway increases with HCHO pressure because it is >1 order in HCHO while the nondeactivating reaction pathway with olefins is only first order in HCHO. When aromatics are co-processed with HCHO and CH₃OH, the site-loss selectivity of HCHO increases with HCHO co-feed pressure because the pathway involving reaction of HCHO with dienic species contributes non-negligibly to the site-loss yield. This also suggests that when co-feeding aromatics with HCHO, most of the HCHO is consumed via nondeactivation pathways, since the site-loss selectivity increases with HCHO pressure (Figure 1c), in agreement with the site-loss selectivities reported for 0.2 kPa HCHO co-feed with various additional co-feeds shown in Figure 2.

The relationship between site-loss yield and HCHO pressure with and without a toluene co-feed is quantitatively similar (Figure 1a), suggesting that the prevailing deactivation mechanism is unchanged by co-feeding toluene. The difference between the site-loss yield with and without C₇H₈ co-feed is positive order in HCHO pressure (Figure 1b). This is rationalized by considering that with or without the aromatic co-feed, the diene-based deactivation pathway dominates, and the selectivity of this pathway increases with increasing HCHO pressure, in agreement with the increasing site-loss selectivity with increasing HCHO co-feed pressure, as observed in Figure 1c. The difference in site-loss yield increases proportionally to HCHO pressure (Figure 1d) because an additional pathway,

the aromatics-based pathway, contributes to deactivation when toluene is co-fed, and the yield of this pathway is first order in HCHO pressure when co-feeding toluene. The nondeactivating pathway is the reaction between HCHO and olefins to form aromatics via diene intermediates, which is also first order in HCHO. Thus, the selectivity of the HCHO + C_7H_8 pathway is nearly invariant with HCHO co-feed pressure, in agreement with the experimental results shown in Figure 1d.

Mechanistic insights into deactivation during catalysis, such as what we proffer for methanol-to-hydrocarbon conversion on zeolites, can be obtained using quantitative metrics that assess the site-averaged rate of deactivation reactions (moles sites lost per second) with respect to the site-averaged rate of reactant/ co-feed consumption (site-loss selectivity) or the molar reactant flow rate (site-loss yield). Specifically, these metrics enable the determination of the dependence of the rate of deactivation pathways on the identity and partial pressures of co-fed reactants, providing experimental evidence in support of plausible HCHO-mediated deactivation pathways during MTH catalysis. By analyzing the dependencies of site-loss yield and selectivity on reactant partial pressures, polyunsaturated nonaromatic species such as aliphatic- or cyclodienes are determined to likely play a critical role in deactivation of zeolite and zeotype catalysts relevant for MTH.

4. CONCLUSIONS

We probe the mechanism of catalyst deactivation during methanol-to-hydrocarbon catalysis on HZSM-5 by measuring site-loss yields and selectivities as functions of reactant composition. Through co-feed experiments, we determine that it is unlikely that the reaction between HCHO and aromatics is the predominant HCHO-mediated deactivation pathway during MTH catalysis on HZSM-5. With a 1.0 kPa toluene co-feed, the site-loss yield was greater than first order in the HCHO co-feed pressure, suggesting that an alternative deactivation pathway requiring multiple species that originate from HCHO contributes non-negligibly to deactivation. We propose that reactions involving polyunsaturated nonaromatic species, such as aliphatic or cyclodienes, are strong candidates for key species that mediate deactivation during MTH catalysis on HZSM-5. This proposal is supported by an increase in the site-loss selectivity of HCHO from 0.002 mol $H_{\rm lost}^+$ mol HCHO⁻¹ when feeding only 0.2 kPa HCHO and 12 kPa CH_3OH to 0.35 mol H_{lost}^+ mol $HCHO^{-1}$ with the addition of 1.0 kPa 1,3-butadiene, while site-loss selectivity only increases to 0.005 mol H_{lost}^+ mol HCHO⁻¹ with the addition of 1.0 kPa toluene.

ASSOCIATED CONTENT

5 Supporting Information

The Supporting Information is available free of charge at https://pubs.acs.org/doi/10.1021/acscatal.0c05335.

Discussion on the analysis of site-loss yields and selectivities in the presence of concentration gradients; methanol conversion as a function of time and contact time with varying co-feeds; methanol conversion and selectivity with and without a 0.2 kPa formaldehyde pretreatment (PDF)

AUTHOR INFORMATION

Corresponding Author

Aditya Bhan — Department of Chemical Engineering and Materials Science, University of Minnesota-Twin Cities, Minneapolis, Minnesota 55455, United States; oorcid.org/0000-0002-6069-7626; Email: abhan@umn.edu; Fax: (+1) 612-626-7246

Authors

Brandon L. Foley — Lawrence Livermore National Laboratory, Livermore, California 94550, United States; Department of Chemical Engineering and Materials Science, University of Minnesota-Twin Cities, Minneapolis, Minnesota 55455, United States

Blake A. Johnson – Department of Chemical Engineering and Materials Science, University of Minnesota-Twin Cities, Minneapolis, Minnesota 55455, United States

Complete contact information is available at: https://pubs.acs.org/10.1021/acscatal.0c05335

Notes

The authors declare no competing financial interest.

ACKNOWLEDGMENTS

We thank Zhichen Shi for helpful technical discussions and for assistance in obtaining experimental data and Neil Razdan for helpful technical discussions. This material is based upon work supported by the National Science Foundation Graduate Research Fellowship under Grant No. 00039202. We also acknowledge the National Science Foundation (CBET 1701534) for financial support. Writing of this manuscript was partially supported under the auspices of the U.S. Department of Energy by Lawrence Livermore National Laboratory under Contract DE-AC52-07NA27344.

REFERENCES

- (1) Haw, J. F.; Song, W.; Marcus, D. M.; Nicholas, J. B. The Mechanism of Methanol to Hydrocarbon Catalysis. *Acc. Chem. Res.* **2003**, *36*, 317–326.
- (2) Olsbye, U.; Svelle, S.; Lillerud, K. P.; Wei, Z. H.; Chen, Y. Y.; Li, J. F.; Wang, J. G.; Fan, W. B. The Formation and Degradation of Active Species during Methanol Conversion over Protonated Zeotype Catalysts. *Chem. Soc. Rev.* **2015**, *44*, 7155–7176.
- (3) Olsbye, U.; Svelle, S.; Bjrgen, M.; Beato, P.; Janssens, T. V. W.; Joensen, F.; Bordiga, S.; Lillerud, K. P. Conversion of Methanol to Hydrocarbons: How Zeolite Cavity and Pore Size Controls Product Selectivity. *Angew. Chem., Int. Ed.* **2012**, *51*, 5810–5831.
- (4) Tian, P.; Wei, Y.; Ye, M.; Liu, Z. Methanol to Olefins (MTO): From Fundamentals to Commercialization. *ACS Catal.* **2015**, *5*, 1922–1938.

- (5) Hwang, A.; Bhan, A. Deactivation of Zeolites and Zeotypes in Methanol-to-Hydrocarbons Catalysis: Mechanisms and Circumvention. *Acc. Chem. Res.* **2019**, 2647–2656.
- (6) Müller, S.; Liu, Y.; Vishnuvarthan, M.; Sun, X.; Van Veen, A. C.; Haller, G. L.; Sanchez-Sanchez, M.; Lercher, J. A. Coke Formation and Deactivation Pathways on H-ZSM-5 in the Conversion of Methanol to Olefins. *J. Catal.* **2015**, 325, 48–59.
- (7) Müller, S.; Liu, Y.; Kirchberger, F. M.; Tonigold, M.; Sanchez-Sanchez, M.; Lercher, J. A. Hydrogen Transfer Pathways during Zeolite Catalyzed Methanol Conversion to Hydrocarbons. *J. Am. Chem. Soc.* **2016**, *138*, 15994–16003.
- (8) Martinez-Espin, J. S.; Mortén, M.; Janssens, T. V. W.; Svelle, S.; Beato, P.; Olsbye, U. New Insights into Catalyst Deactivation and Product Distribution of Zeolites in the Methanol-to-Hydrocarbons (MTH) Reaction with Methanol and Dimethyl Ether Feeds. *Catal. Sci. Technol.* **2017**, *7*, 2700–2716.
- (9) Rojo-Gama, D.; Mentel, L.; Kalantzopoulos, G. N.; Pappas, D. K.; Dovgaliuk, I.; Olsbye, U.; Lillerud, K. P.; Beato, P.; Lundegaard, L. F.; Wragg, D. S.; Svelle, S. Deactivation of Zeolite Catalyst H-ZSM-5 during Conversion of Methanol to Gasoline: Operando Time- and Space-Resolved X-Ray Diffraction. *J. Phys. Chem. Lett.* **2018**, *9*, 1324—1328.
- (10) Arora, S. S.; Bhan, A. The Critical Role of Methanol Pressure in Controlling Its Transfer Dehydrogenation and the Corresponding Effect on Propylene-to-Ethylene Ratio during Methanol-to-Hydrocarbons Catalysis on H-ZSM-5. *J. Catal.* **2017**, *356*, 300–306.
- (11) Hwang, A.; Bhan, A. Bifunctional Strategy Coupling Y₂O₃-Catalyzed Alkanal Decomposition with Methanol-to-Olefins Catalysis for Enhanced Lifetime. *ACS Catal.* **2017**, *7*, 4417–4422.
- (12) Hwang, A.; Kumar, M.; Rimer, J. D.; Bhan, A. Implications of Methanol Disproportionation on Catalyst Lifetime for Methanol-to-Olefins Conversion by HSSZ-13. *J. Catal.* **2017**, *346*, 154–160.
- (13) Guisnet, M.; Magnoux, P. Organic Chemistry of Coke Formation. *Appl. Catal.*, A **2001**, 212, 83–96.
- (14) Guisnet, M.; Ribeiro, F. R. Deactivation and Regeneration of Zeolite Catalysts; Hutchings, G. J., Ed.; Imperial College Press: London, 2011; pp 115–130.
- (15) Rojo-Gama, D.; Signorile, M.; Bonino, F.; Bordiga, S.; Olsbye, U.; Lillerud, K. P.; Beato, P.; Svelle, S. Structure—Deactivation Relationships in Zeolites during the Methanol—to-Hydrocarbons Reaction: Complementary Assessments of the Coke Content. *J. Catal.* **2017**, 351, 33—48.
- (16) Pinilla-Herrero, I.; Olsbye, U.; Márquez-Álvarez, C.; Sastre, E. Effect of Framework Topology of SAPO Catalysts on Selectivity and Deactivation Profile in the Methanol-to-Olefins Reaction. *J. Catal.* **2017**, 352, 191–207.
- (17) Goetze, J.; Meirer, F.; Yarulina, I.; Gascon, J.; Kapteijn, F.; Ruiz-Martínez, J.; Weckhuysen, B. M. Insights into the Activity and Deactivation of the Methanol-to-Olefins Process over Different Small-Pore Zeolites As Studied with Operando UV-Vis Spectroscopy. *ACS Catal.* **2017**, *7*, 4033–4046.
- (18) Park, J. W.; Lee, J. Y.; Kim, K. S.; Hong, S. B.; Seo, G. Effects of Cage Shape and Size of 8-Membered Ring Molecular Sieves on Their Deactivation in Methanol-to-Olefin (MTO) Reactions. *Appl. Catal., A* **2008**, 339, 36–44.
- (19) Martinez-Espin, J. S.; De Wispelaere, K.; Westgård Erichsen, M.; Svelle, S.; Janssens, T. V. W.; Van Speybroeck, V.; Beato, P.; Olsbye, U. Benzene Co-Reaction with Methanol and Dimethyl Ether over Zeolite and Zeotype Catalysts: Evidence of Parallel Reaction Paths to Toluene and Diphenylmethane. *J. Catal.* **2017**, 349, 136–148.
- (20) Foley, B. L.; Bhan, A. Transient and Steady-State Kinetic Studies of Formaldehyde Alkylation of Benzene to Form Diphenylmethane on HZSM-5 Catalysts. *ACS Catal.* **2020**, *10*, 10436—10448. (21) Anderson, J. R.; Chang, Y. F.; Western, R. J. Retained and Desorbed Products from Reaction of 1-Hexene over H-ZSM5 Zeolite: Routes to Coke Precursors. *J. Catal.* **1989**, *118*, 466–482.

- (22) Anderson, J. R.; Chang, Y. F.; Western, R. J. The Effect of Acidity on the Formation of Retained Residue From-1-Hexene over Usy Zeolite Catalysts. *Stud. Surf. Sci. Catal.* **1991**, *68*, 745–751.
- (23) Barbier, J. Deactivation of Reforming Catalysts by Coking a Review. *Appl. Catal.* **1986**, 23, 225–243.
- (24) Guisnet, M.; Costa, L.; Ribeiro, F. R. Prevention of Zeolite Deactivation by Coking. J. Mol. Catal. A: Chem. 2009, 305, 69-83.
- (25) Lezcano-Gonzalez, I.; Campbell, E.; Hoffman, A. E. J.; Bocus, M.; Sazanovich, I. V.; Towrie, M.; Agote-Aran, M.; Gibson, E. K.; Greenaway, A.; De Wispelaere, K.; Van Speybroeck, V.; Beale, A. M. Insight into the Effects of Confined Hydrocarbon Species on the Lifetime of Methanol Conversion Catalysts. *Nat. Mater.* **2020**, *19*, 1081–1087.
- (26) Sushkevich, V. L.; Ordomsky, V. V.; Ivanova, I. I. Synthesis of Isoprene from Formaldehyde and Isobutene over Phosphate Catalysts. *Appl. Catal., A* **2012**, 441–442, 21–29.
- (27) Arundale, E.; Mikeska, L. A. The Olefin-Aldehyde Condensation. The Prins Reaction. *Chem. Rev.* **1952**, *51*, 505–555.
- (28) Adams, D. R.; Bhatnagar, S. P. The Prins Reaction. *Synthesis* **1977**, 1977, 661–672.
- (29) Chua, Y. T.; Stair, P. C. An Ultraviolet Raman Spectroscopic Study of Coke Formation in Methanol to Hydrocarbons Conversion over Zeolite H-MFI. *J. Catal.* **2003**, *213*, 39–46.
- (30) Haw, J. F.; Nicholas, J. B.; Song, W.; Deng, F.; Wang, Z.; Xu, T.; Heneghan, C. S. Roles for Cyclopentenyl Cations in the Synthesis of Hydrocarbons from Methanol on Zeolite Catalyst HZSM-5. *J. Am. Chem. Soc.* **2000**, 122, 4763–4775.
- (31) Wang, C.; Xu, J.; Qi, G.; Gong, Y.; Wang, W.; Gao, P.; Wang, Q.; Feng, N.; Liu, X.; Deng, F. Methylbenzene Hydrocarbon Pool in Methanol-to-Olefins Conversion over Zeolite H-ZSM-5. *J. Catal.* **2015**, 332, 127–137.
- (32) Hazra, M. K.; Francisco, J. S.; Sinha, A. Gas Phase Hydrolysis of Formaldehyde to Form Methanediol: Impact of Formic Acid Catalysis. *J. Phys. Chem. A* **2013**, *117*, 11704–11710.
- (33) Wang, C.; Hu, M.; Chu, Y.; Zhou, X.; Wang, Q.; Qi, G.; Li, S.; Xu, J.; Deng, F. π-Interactions between Cyclic Carbocations and Aromatics Cause Zeolite Deactivation in Methanol-to-Hydrocarbon Conversion. *Angew. Chem., Int. Ed.* **2020**, *59*, 7198–7202.
- (34) Ipatieff, V. N.; Pines, H.; Schaad, R. E. Reaction of Benzene with Butadiene in the Presence of Sulfuric Acid and Hydrogen Fluoride Catalysts. *J. Am. Chem. Soc.* **1944**, *66*, 816–817.
- (35) Ipatieff, V. N.; Schaad, R. E.; Pines, H.; Monroe, G. S. Reaction between Benzene and Butadiene in the Presence of Silico-Phosphoric Acid Catalyst. *J. Am. Chem. Soc.* **1945**, *67*, 1060–1062.
- (36) Rojo-Gama, D.; Etemadi, S.; Kirby, E.; Lillerud, K. P.; Beato, P.; Svelle, S.; Olsbye, U. Time- and Space-Resolved Study of the Methanol to Hydrocarbons (MTH) Reaction-Influence of Zeolite Topology on Axial Deactivation Patterns. *Faraday Discuss.* **2017**, *197*, 421–446
- (37) Foley, B. L.; Johnson, B. A.; Bhan, A. A Method for Assessing Catalyst Deactivation: A Case Study on Methanol-to-Hydrocarbons Conversion. *ACS Catal.* **2019**, *9*, 7065–7072.
- (38) Chen, D.; Rebo, H. P.; Moljord, K.; Holmen, A. Influence of Coke Deposition on Selectivity in Zeolite Catalysis. *Ind. Eng. Chem. Res.* 1997, 36, 3473–3479.
- (39) Janssens, T. V. W. A New Approach to the Modeling of Deactivation in the Conversion of Methanol on Zeolite Catalysts. *J. Catal.* **2009**, *264*, 130–137.
- (40) Ilias, S.; Khare, R.; Malek, A.; Bhan, A. A Descriptor for the Relative Propagation of the Aromatic- and Olefin-Based Cycles in Methanol-to-Hydrocarbons Conversion on H-ZSM-5. *J. Catal.* **2013**, 303, 135–140.
- (41) Khare, R.; Millar, D.; Bhan, A. A Mechanistic Basis for the Effects of Crystallite Size on Light Olefin Selectivity in Methanol-to-Hydrocarbons Conversion on MFI. *J. Catal.* **2015**, *321*, 23–31.
- (42) Teketel, S.; Olsbye, U.; Lillerud, K. P.; Beato, P.; Svelle, S. Co-Conversion of Methanol and Light Alkenes over Acidic Zeolite Catalyst H-ZSM-22: Simulated Recycle of Non-Gasoline Range Products. *Appl. Catal., A* **2015**, 494, 68–76.

- (43) Sun, X.; Mueller, S.; Liu, Y.; Shi, H.; Haller, G. L.; Sanchez-Sanchez, M.; Van Veen, A. C.; Lercher, J. A. On Reaction Pathways in the Conversion of Methanol to Hydrocarbons on HZSM-5. *J. Catal.* **2014**, *317*, 185–197.
- (44) Vasiliadou, E. S.; Gould, N. S.; Lobo, R. F. Zeolite-Catalyzed Formaldehyde–Propylene Prins Condensation. *ChemCatChem* **2017**, 9, 4417–4425.
- (45) Arora, S. S.; Shi, Z.; Bhan, A. Mechanistic Basis for Effects of High-Pressure H2 Cofeeds on Methanol-to-Hydrocarbons Catalysis over Zeolites. *ACS Catal.* **2019**, *9*, 6407–6414.
- (46) Arora, S. S.; Nieskens, D. L. S.; Malek, A.; Bhan, A. Lifetime Improvement in Methanol-to-Olefins Catalysis over Chabazite Materials by High-Pressure H₂ Co-Feeds. *Nat. Catal.* **2018**, *1*, 666–672
- (47) DeLuca, M.; Janes, C.; Hibbitts, D. Contrasting Arene, Alkene, Diene, and Formaldehyde Hydrogenation in H-ZSM-5, H-SSZ-13, and H-SAPO-34 Frameworks during MTO. ACS Catal. 2020, 10, 4593–4607.
- (48) Liu, Y.; Kirchberger, F. M.; Müller, S.; Eder, M.; Tonigold, M.; Sanchez-Sanchez, M.; Lercher, J. A. Critical Role of Formaldehyde during Methanol Conversion to Hydrocarbons. *Nat. Commun.* **2019**, *10*, No. 1462.
- (49) Chang, C. D.; Silvestri, A. J. The Conversion of Methanol and Other O-Compounds to Hydrocarbons over Zeolite Catalysts. *J. Catal.* **1977**, 47, 249–259.
- (50) Dermer, O. C.; Kohn, L.; Nelson, W. J. The Reaction of 1,3-Butadiene with Formaldehyde. *J. Am. Chem. Soc.* **1951**, 73, 5869–5870.
- (51) Hutchings, G. J.; Hunter, R. Hydrocarbon Formation from Methanol and Dimethyl Ether: A Review of the Experimental Observations Concerning the Mechanism of Formation of the Primary Products. *Catal. Today* **1990**, *6*, 279–306.